Liquid Crystals
Publication details, including instructions for authors and subscription information:
http://www.informaworld.com/smpp/title~content=t713926090

Ribbon phases in surfactant systems Comparisons between experimental results and predictions of a theoretical model

Håkan Hagslätt[a]; Olle Söderman[a]; Bengt Jönsson[a]
[a] Department of Physical Chemistry 1, Chemical Centre, University of Lund, Lund, Sweden

To cite this Article Hagslätt, Håkan , Söderman, Olle and Jönsson, Bengt(1994) 'Ribbon phases in surfactant systems Comparisons between experimental results and predictions of a theoretical model', Liquid Crystals, 17: 2, 157 — 177
To link to this Article: DOI: 10.1080/02678299408036557
URL: http://dx.doi.org/10.1080/02678299408036557

LIQUID CRYSTALS, 1994, VOL. 17, NO. 2, 157–177

Ribbon phases in surfactant systems

Comparisons between experimental results and predictions of a theoretical model

by HÅKAN HAGSLÄTT*, OLLE SÖDERMAN and BENGT JÖNSSON
Department of Physical Chemistry 1, Chemical Centre, University of Lund, P.O.B. 124, S-221 00 Lund, Sweden

(*Received 15 April, 1993; accepted 25 June 1993*)

Ribbon phases consist of long cylindrical aggregates that have non-circular normal sections. We have recently pointed out that scattering data for a large number of different intermediate ribbon phases of lower than hexagonal symmetry found in ionic surfactant systems indicate that these phases have a structure possessing a centred rectangular symmetry. In this communication, we have investigated the aggregate dimensions for the phases with cylindrical aggregates, i.e., the hexagonal phases and the centred rectangular ribbon phases. Previously published phase diagrams, small angle X-ray and neutron scattering data and ^{2}H NMR data for these phases in different systems have been used for this purpose. The results are that the axial ratios of the aggregates increase when the temperature decreases, when the surfactant concentration increases, and when the average surfactant charge decreases. Models that semi-quantitatively describe the thermodynamics of the micellar, hexagonal and lamellar phases, which are based on the Poisson–Boltzmann cell model approach, have previously been presented in the literature. We have extended these models to treat also the ribbon phases. The results from the calculations show the same trends with respect to changes in the dimensions of the non-circular aggregates upon changes in temperature, surfactant concentration and average surfactant charge, as those obtained experimentally. Theoretically calculated phase diagrams with ribbon phases are also presented. Based on the predictions of the model and some previously published experimental data for hexagonal phases, it is proposed that the formation of non-circular, cylindrical aggregates is a general property of single-chain, ionic surfactant/water systems, and that these aggregates in general pack on hexagonal lattices. The normal sections of these aggregates are circular on average, on account of the fact that the degree of deformation and the orientation of deformation changes along the axis of the aggregates and with time. Only for some systems, temperatures and surfactant concentrations do the asymmetric aggregates line up and ribbon phases with centred rectangular symmetry are obtained. The driving mechanisms for the transition from the hexagonal phase with asymmetric (fluctuating) cylinders and further to the centred rectangular phase with asymmetric (stiff) cylinders is also discussed. It is argued that this phase transition is of the first order.

1. Introduction

When amphiphilic molecules are mixed with water and/or hydrocarbons, a whole hierarchy of different aggregates are formed, of which the most well-known are the ones that result in micellar solution phases (spheres), hexagonal phases (extended circular cylinders) or lamellar phases (extended bilayers). The micellar and hexagonal phases may be of either the normal type, with the surfaces of the aggregates curved towards the

* Author for correspondence.

0267–8292/94 $10·00

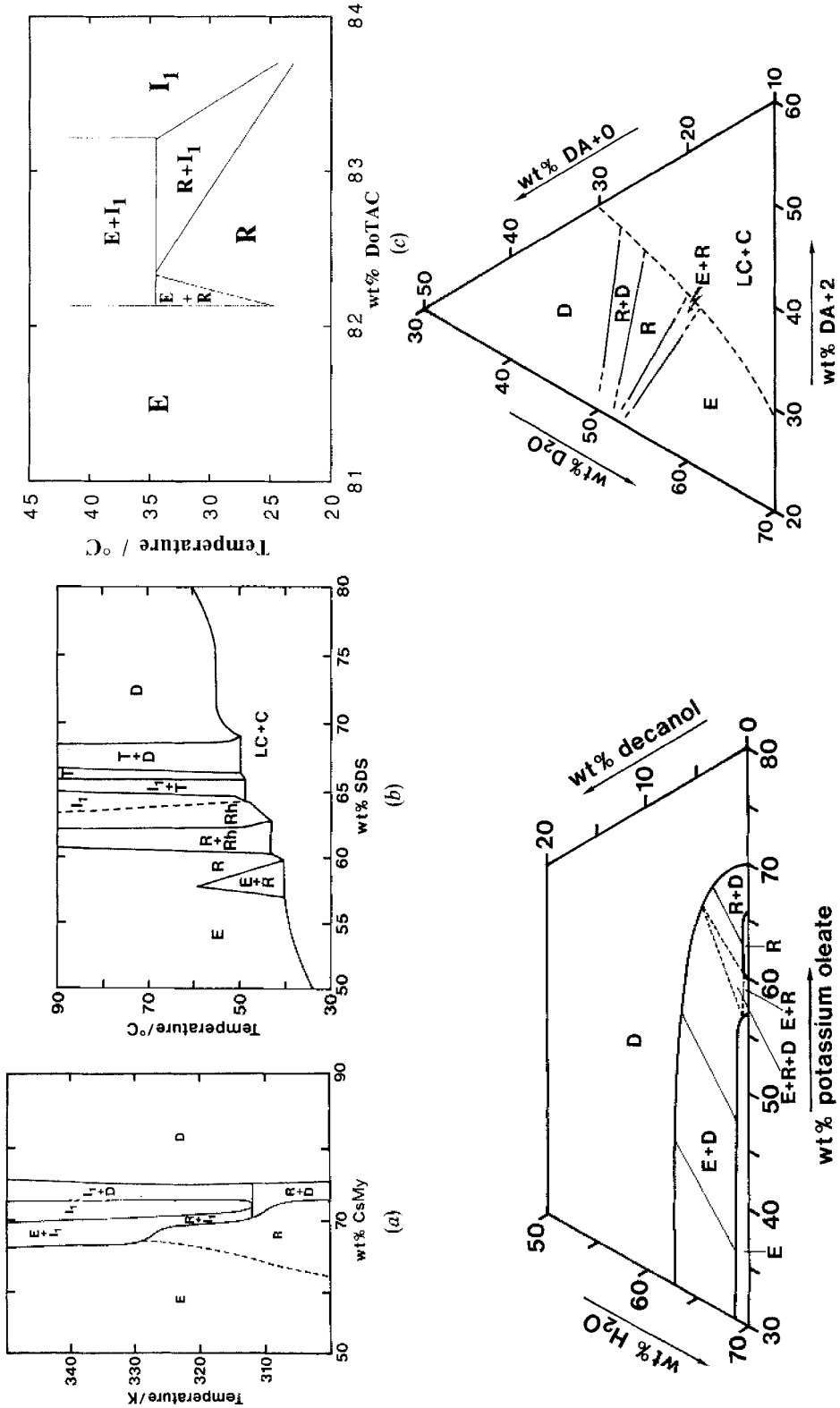

Figure 1. Redrawn phase diagrams for (*a*) $CsMy/D_2O$ from [24] (note that the space group of the R phase of this system has not been investigated), (*b*) SDS/H_2O from [39], (*c*) $DoTAC/H_2O$ from [22], (*d*) $KO/dec/H_2O$ at 20°C from [14] and (*e*) DA(+2)/DA (+0)/D_2O at 25°C from [40]. E denotes hexagonal phases, R rectangular phases, Rh rhombohedral phases, I_1 bicontinuous cubic phases, T tetragonal phases, D lamellar phases and LC+C denotes liquid crystalline phases plus hydrated surfactant crystals.

hydrocarbon, or of the reversed type, with curvature towards the water. However, several other phases have been found as well, especially in regions between the hexagonal and the lamellar phases, and these phases are generally called 'intermediate phases' [1, 2]. The rhombohedral phase [3], the tetragonal phase [3–5], the bicontinuous cubic phases [6] and the ribbon phases [1, 2, 7] all belong to this group, of which the cubic phases and the ribbon phases seem to be the most common ones for systems with charged surfactants. Some phase diagrams that include ribbon phases are shown in figure 1 (the abbreviations of the amphiphilic compounds are given in table 1). Ribbon phases consist of elongated non-circular cylinders that are packed on two-dimensional lattices. Actually, the term 'ribbon phase' [8] is merely to be considered as a collective name for several different phases, which, for example, can be of rectangular symmetries (of space groups pmm, pgg and cmm) or of oblique symmetry (space group p2), see figure 2. It is evident that the extension of ribbon phases is often quite limited

Table 1. List of abbreviations for surfactants and co-surfactants.

Abbreviation	System
KO	Potassium oleate
KP	Potassium palmitate
CsMy	Caesium myristate
KL	Potassium laurate
SDS	Sodium dodecylsulphate
SdS	Sodium decylsulphate
DoTAC	Dodecyltrimethylammonium chloride
DoPDA	Dodecyl-1,3-propylene-bisamine (DA + 0)
DoPDAC	Dodecyl-1,3-propylene-bisammonium chloride (DA + 2)
DA + z	Dodecyl-1,3-propylene-diamine + z HCl, $0 \leqslant z \leqslant 2$.
dec	1-decanol

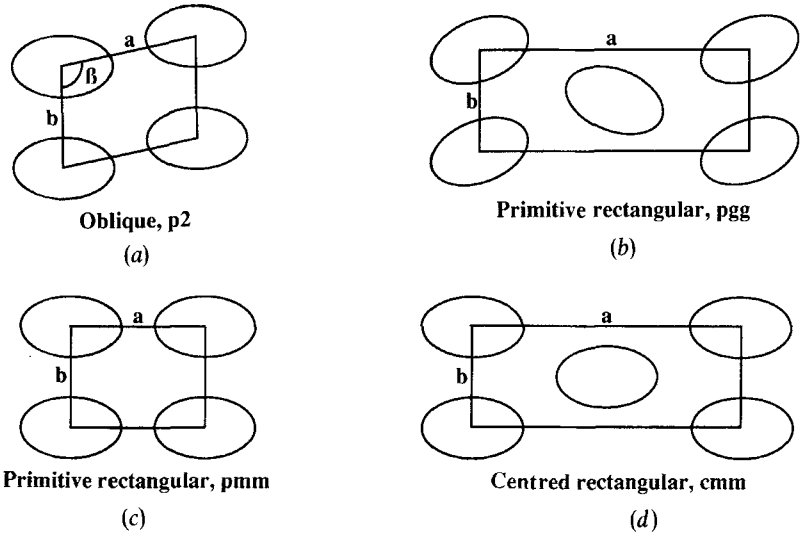

Figure 2. Phase structures for ribbon phases. The two-dimensional space groups are (*a*) p2, (*b*) pgg, (*c*) pmm and (*d*) cmm, and *a* and *b* are unit cell dimensions and β is unit cell angle.

with respect to composition and/or temperature, and therefore there are probably several already investigated surfactant systems with as yet undiscovered ribbons phases.

To increase our general understanding regarding the mechanisms which govern surfactant self-assembly, it is important to understand under what conditions ribbon phases are formed. One way of obtaining such an understanding is to resort to theoretical modelling. It is a formidable task to model all the interactions in a multi-component surfactant system. Nonetheless, one has a good theoretical understanding of the formation of the micellar solution phases, the hexagonal phases with circular cylindrical aggregates and the lamellar phase, especially for systems with ionic surfactants, for which one of the present authors and co-workers have developed models, based on the Poisson–Boltzmann cell model approach [9–12].

In this work, we have extended this model so that ribbon phases are also treated. A centred rectangular packing of the aggregates is used (figure 2), in agreement with the experimental results [7]. It should be remarked that one thermodynamic model that aims at describing the temperature dependence on the shape of the ribbon-like aggregates has been presented [13]. However, this model describes the different energies of the system less quantitatively, and is also less general than the model presented here.

The disposition of this paper is as follows. We start by presenting some experimental results pertaining to ribbon phases. In particular, some phase diagrams where ribbon phases appear will be shown and the dimensions of the normal section of the ribbon-like aggregates, evaluated within the frame-work of a particular model, the hexagon-rod model, will be presented. Subsequently, the Poisson–Boltzmann cell model and its derived predictions will be presented. These predictions are phase diagrams and the dimensions of the normal sections of the aggregates. The model calculations indicate some important aspects concerning the aggregate structure in phases of hexagonal symmetry close to the transition from the hexagonal to the adjacent phase at higher surfactant concentration. A discussion about this feature and its implications for the phase transition between phases of hexagonal and rectangular symmetries terminates the paper. To make the presentation clearer we have relegated some sections to appendices.

2. Experimental results

2.1. *Phase diagrams with ribbon phases*

Ribbon phases have been found in several different systems comprised of ionic, single chained surfactants and water [1–3, 7, 14–25]. Phase diagrams have been obtained for some of these systems, of which the most well characterized ones are represented in figure 1.

2.2. *The symmetry of the ribbon phases*

Luzzati *et al.*, provided the first evidence in favour of ribbon phases in 1960, by small angle X-ray scattering (SAXS) measurements [1, 2]. Rectangular phases were subsequently obtained for the binary surfactant/water systems with potassium oleate, sodium oleate, potassium palmitate and potassium laurate. The first direct proof for the existence of the ribbon-like aggregates was obtained by Doane *et al.*, who performed ^{2}H NMR measurements on the potassium palmitate/potassium laurate/water system [15, 26]. They obtained non-zero asymmetry parameters in the ^{2}H band shape from the intermediate phase and their interpretation was that the phase consisted of ribbon-like aggregates.

Primitive rectangular (pmm) [1, 2, 14, 16], primitive rectangular (pgg) [17, 18], centred rectangular (cmm) [7, 19–22], and oblique [3, 23] symmetries have all been proposed for ribbon phases (figure 2). However, we have investigated the question of the symmetry or ribbon phases in a previous paper [7], and it was concluded that a centred rectangular symmetry (cmm) was consistent with all published scattering data for these phases. For no scattering data set were the pgg, pmm or p2 symmetries favoured over the cmm symmetry. It deserves to be mentioned that there is some recent evidence for the existence of a primitive rectangular (pgg) ribbon phase in the sodium decylsulphate/1-decanol/water system, in addition to a centred rectangular ribbon phase [27].

We have previously discussed the matter of symmetry of the ribbon phases from a theoretical point of view, and the result was that the cmm symmetry is favoured over the p2, pmm and pgg symmetries [7]. In short the arguments were as follows; when modelling a liquid crystalline phase, one should preferably consider the shape, the spacing and the orientation of the aggregates. Experimental, as well as theoretical, results show that it is energetically favourable to maintain a constant thickness of the water layer that separates the aggregates in the system [11], and to form simultaneously aggregates where the hydrophilic/hydrophobic interfacial area is at a minimum. The latter condition has to be fulfilled with some additional constraints, such as for example that the smallest dimension of the aggregates must not exceed a certain critical value. For a system consisting of ribbon-like aggregates, these conditions are well fulfilled in a cell model where the cells and the aggregates are approximated by 'stretched hexagons' for which all angles are 120°, and with a constant thickness of the water layer in the cells—the hexagon–rod model which is presented in figure 3. Filling the space with these cells results in a phase with cmm symmetry.

To conclude, it appears that the ribbon phases are in general of the centred rectangular type (cmm). Other symmetries are possible as well, and it would be surprising if some of these were not to be found in the future. Nevertheless, since the centred rectangular symmetry is the clearly predominant one for ribbon phases with lower than hexagonal symmetry, we will in what follows assume a centred rectangular structure for these phases.

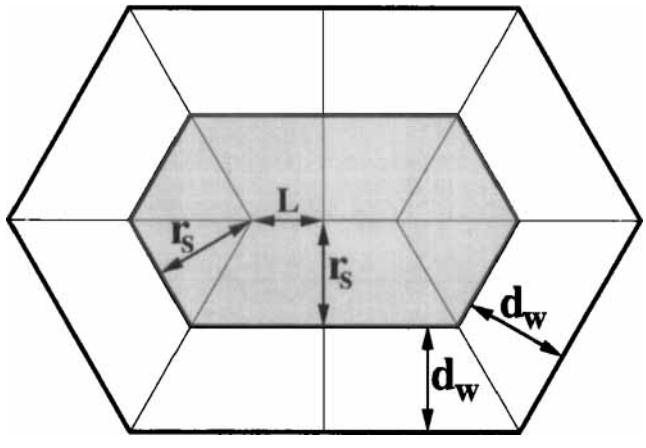

Figure 3. The hexagon–rod model [7]. The thickness of the water layer is constant, d_w. L is the half length of the lamellar-like region and r_s is the smallest dimension of the aggregate.

2.3. *The dimensions of the aggregates of the ribbon phases*

We have previously evaluated the aggregate dimensions for the ribbon phases in nine different systems [7] (from SAXS or ^{2}H NMR data) and it was concluded that the axial ratio of the aggregate normal sections, ρ, defined as the ratio of the major and minor axes, are bigger than 1·2 : 1 and smaller than 2 : 1 for these systems, and that the smallest dimension of the aggregates (r_s) is about 80 per cent of the length of the all-*trans*-conformation of the surfactant (l_{at}). Moreover, the ribbon phases have rather limited extensions with respect to temperature and/or surfactant concentration (figure 1), and one would therefore expect small changes of the dimensions of the aggregates within the ribbon phases. That this is indeed the case is shown in figures 4 and 5, where the results from previously obtained SAXS and ^{2}H NMR data are given. The SAXS data have been evaluated by use of the hexagon–rod model [7], and, for reasons of consistency, the NMR data have been evaluated using the same shape of the aggregate normal section. Unless otherwise stated, the resulting axial ratios are for the hydrocarbon core of the aggregates. The procedure for obtaining these data with the hexagon–rod model is described in appendices A and B.

A slight increase of the axial ratio of the aggregates, corresponding to a decrease of the area available per surfactant headgroup (A_{sp}), when the surfactant concentration increases, is noted (at least for the DA + 1/water and the DoTAC/water systems), cf. figure 4. This observation is reasonable, since the counter-ion screening of the electrostatic potential of the aggregate surface increases when the surfactant concentration increases, and therefore the headgroups get closer packed in order to reduce the hydrocarbon/water contact area.

The aggregate shape is strongly dependent on the temperature for many non-ionic systems, but for charged systems with water as the solvent, the situation is the opposite, especially at temperatures around room-temperature [9, 28]. A slight decrease of the

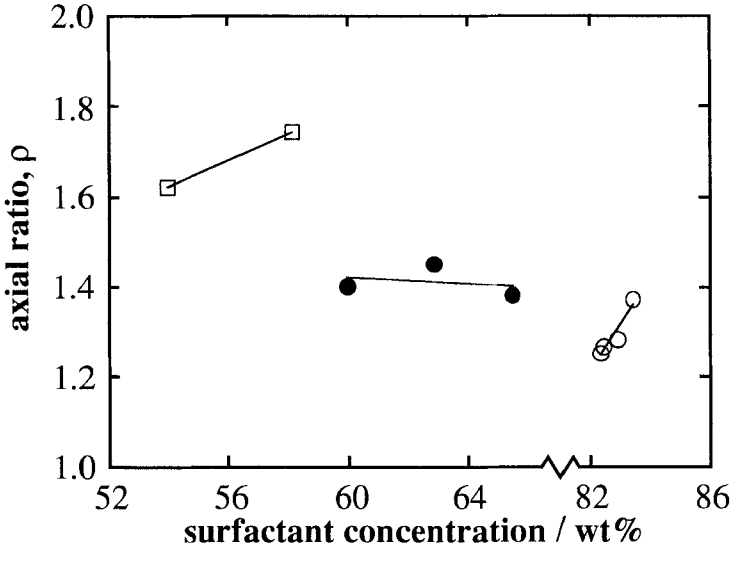

Figure 4. Axial ratios of the aggregates' normal sections as a function of the surfactant concentration for the (□) DA(+1)/D_2O system at 25°C (SAXS), (●) the KO/H_2O system at 20°C (SAXS) and (○) the DoTAC/H_2O system at 24°C (^{2}H NMR). The axial ratios are at the headgroups for the DoTAC/H_2O case. The lines are drawn only to facilitate the reading of the data. The raw data are taken from [7, 14 and 22], respectively.

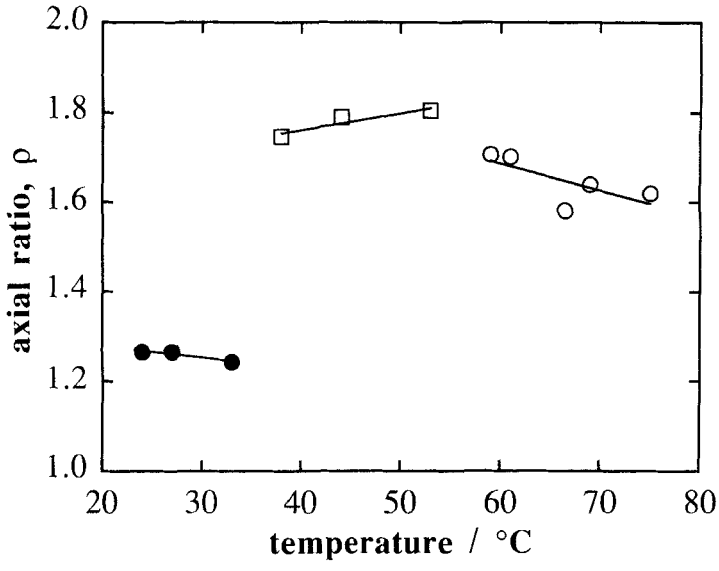

Figure 5. Axial ratios of the aggregates' normal sections as a function of the temperature for the (●) DoTAC/H_2O system with 82·5 wt.% DoTAC (^{2}H NMR), (□) the KP/KL/H_2O system with about 55·0 wt.% KP and 6·2 wt.% KL (^{2}H NMR) and (○) the KP/H_2O system with 59 wt.% KP (SAXS). The axial ratios are at the headgroups for the DoTAC case. The lines are drawn only to facilitate the reading of the data. The raw data are taken from [22 and 41], [38] and [16], respectively.

Table 2. Aggregate axial ratios for the KP/KL/H_2O system as obtained from ^{2}H NMR measurements and the hexagon–rod model. The composition of the sample is approximately 55·0 wt.% KP and 6·2 wt.% KL. The notation is as defined in the text.

T/°C*	X(KL)†	η(KL)†	η(KP)†	ρ	X(KL)e	X(KL)c
38	0·12	0·2	1·0	1·75	0·16	0·085
44	0·12	0·5	1·0	1·79	0·15	0·098
53	0·12	0·6	1·0	1·81	0·14	0·10

† Data taken from [38].

axial ratio of the aggregates when the temperature increases is noted for the KP/water and the DoTAC/water systems (figure 5). The increase of the axial ratio of the KP/KL aggregates may be an effect of a larger uncertainty in the data for this case, but there is another reasonable interpretation. The fraction of potassium laurate at the triangular (edge) parts of the hexagon, X(KL)e, is higher than the fraction at the tetragonal parts, X(KL)c (table 2). Such non-uniform surfactant distribution is entropically unfavourable, and therefore more uniform distributions are obtained when the temperature increases. The axial ratio of the aggregates may then increase, since the thickness of the lamellar-like parts of the aggregates decreases when X(KL)c increases, since the laurate molecule is shorter than the palmitate molecule.

The surfactant charge has been varied for two systems (figure 6 and table 3). In neither case does the axial ratio of the aggregates seem to be affected considerably by the average charge of the amphiphilic molecules. In the case of DA/HCl/water, the axial ratio of the aggregates is approximately independent of the surfactant charge along a

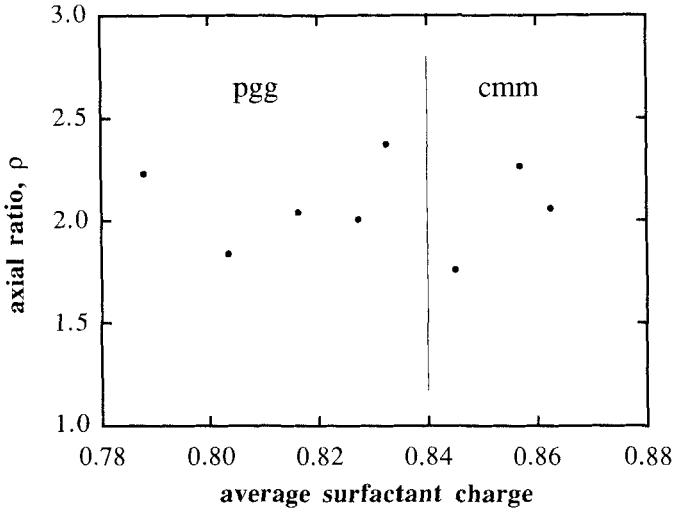

Figure 6. Axial ratios of the aggregates' normal sections as a function of the surfactant average charge for the SdS/dec/H_2O system at 23°C (SAXS). The samples contain about 47·6 wt.% H_2O. The raw data are from [27], and the hexagon–rod model is used for the evaluation of all data sets.

Table 3. Aggregate axial ratios for the DA($+z$)/D_2O system as obtained from SAXS measurements and the hexagon–rod model, taken from [7].

c/wt.%	z	r_s Å	ρ
60·0	1·11	13·5	1·67
54·0	1·02	13·6	1·62
58·2	1·02	13·3	1·74
50·5	0·81	12·9	1·73

line in the phase diagram on which both the surfactant concentration and the average surfactant charge increases. Following such a line (with decreasing water content), the surface charge density of the aggregates increases, but the counter-ion concentration in the system increases as well. Therefore, one would expect small changes of the electrostatic surface potential of the aggregates along the line. Thus, the observed, constant axial ratios of the aggregates of the DA/HCl/water system seem reasonable. For the SdS/dec/water system, the situation is different; the axial ratio of the aggregates is apparently independent of the surfactant average charge along a line in the phase diagram on which the surfactant concentration is constant. On the other hand, the scattering in the data is considerable for this case. In addition, it is unclear from the paper whether the asymmetry parameters in the ^2H NMR spectra from deuteriated 1-decanol and decylsulphate are non-zero for the samples from the ribbon phases.

2.4. *Summary of the experimental results*

The main features of the experimentally obtained results are summarized in table 4. All the conclusions made are valid regardless of the symmetry of the ribbon phase, but we have assumed a centred rectangular symmetry (cmm) for the ribbon phase in table 4, since this structure appears to be the most favoured one [7].

Table 4. Summary of the experimentally and theoretically obtained results for the transition from the hexagonal phase (p6m) to the lamellar phase (linear) via the centred rectangular phase (cmm).

Experimental results			Theoretical results	
comments	phase		phase	comments
{1} Circular cylinders are formed initially {2} The radius of the cylinders increases when the surfactant concentration increases	p6m		p6m	{1} Circular cylinders are formed initially {2} The radius of the cylinders increases when the surfactant concentration increases
{3} *The p6m/cmm transition is of the first order* †				{3} *The p6m/cmm transition is of higher order than the first order*
{4} The cylinders are non-circular {5} The axial ratio of the cylinders are quite small, between 1.2:1 and 2:1 {6} The axial ratio of the aggregates increases slightly when the surfactant concentration increases, when the temperature decreases and when the average surfactant charge decreases {7} *The cmm phase extend over a region of a few weight percent, at surfactant concentrations c ≥ 50 wt%* {8} *This concentration range decreases when the temperature increases, and finally the cmm phase disappears* {9} *The cmm phase is not obtained for all systems*	p6m p6m + cmm cmm	surfactant concentration	cmm	{4} The cylinders are non-circular {5} The axial ratio of the cylinders are quite small, typically smaller than 2:1 {6} The axial ratio of the aggregates increases slightly when the surfactant concentration increases, when the temperature decreases and when the average surfactant charge decreases {7} *The cmm phase forms already at low surfactant concentrations and extends over a large region of concentration* {8} *There is a cmm phase at all temperatures* {9} *The formation of a cmm phase is a general feature, occurring for all systems*
{10} The cmm/lamellar transition is of the first order {11} The width of the two-phase region is a few wt%	cmm + linear		cmm + linear	{10} The cmm/lamellar transition is of the first order {11} The width of the two-phase region is a few wt%
{12} The higher the surfactant charge, the higher the concentration for which the lamellar phase is formed	linear ‡		linear	{12} The higher the surfactant charge, the higher the concentration for which the lamellar phase is formed

† No two-phase region has been observed for the SDS/water system at elevated temperatures and for the CsMy/water system (see Figure 1).
‡ Cubic, tetragonal and/or rhombohedral phases are obtained between the ribbon phase and the lamellar phase for some systems (see Figure 1).

3. A thermodynamic model for ribbon phases

We will investigate three-component systems with water, surfactant and cosurfactant, which are allowed to form circular cylinders, non-circular cylinders and bilayers. To describe these complicated systems in detail is a tremendous task, and as a consequence one needs to model the system in a simplistic manner. Nevertheless, it is possible to predict the trends of different phase diagrams nearly quantitatively by use of models that are based on the Poisson–Boltzmann cell model approach. The models of the hexagonal and lamellar phases are treated in detail in a number of papers by Jönsson and co-workers [9–12] and we will use the results of this work in order to develop a model that treats also the ribbon phases.

We present below the cell model approximations for the three geometries that are considered, and the simplifications imposed on the systems are also introduced. The systems treated consist of surfactant and cosurfactant molecules that are of equal length, and water. In the next section, we will consider the different contributions to the free energy of the systems that are taken into account in the model. In what follows, we present the basic assumptions pertaining to the Poisson–Boltzmann cell model:

(i) The circular cylindrical aggregates are approximated by infinitely long cylinders with symmetric, hexagon-like, normal sections. The aggregate radius is smaller than, or equal to, a certain given maximum length, r_{max}. This approximation corresponds to the representation in figure 3, with the restriction that the half length of the lamellar-like region, L, is equal to zero.

(ii) The aggregates with non-circular normal sections are represented as in the hexagon–rod model (figure 3), i.e., the aggregates are approximated by infinitely long cylinders with the normal section of an extended hexagon, with all angles at 120°. The smallest dimension of the aggregates, r_s, equals r_{max}, whereas $L>0$.

(iii) The bilayers are of infinite extension in two dimensions and are assumed to be totally flat. The thickness of the bilayers is smaller than, or equal to, $2\cdot r_{max}$.

(iv) For all three geometries the surrounding water-layer is of constant thickness, and the aggregates are assumed to be mono-disperse in shape and size. The interior of all aggregates are modelled as a pure liquid hydrocarbon, free from water molecules and counter-ions, and the headgroups of the amphiphilic molecules are confined to be at the surface of the aggregates.

3.1. *The thermodynamic model*

An important contribution to the free energy of ionic surfactant systems is given by the electrostatic interactions between the ions, and we will use the Poisson–Boltzmann equation to describe these interactions. The term describing the energy of the system is

$$E_{el}=\frac{1}{2}\int \rho\Phi dV=\frac{1}{2}\varepsilon_0\varepsilon_r\int(\nabla\Phi)^2\,dV \tag{1}$$

and the term that describes the entropy of mixing of the ions in the water region is

$$-TS_{mix}=N_A kT\int c_i\left(\ln\frac{c_i}{c_0}-1\right)dV \tag{2}$$

where ρ is the charge density, Φ the electrostatic potential, ε_0 the permittivity in a vacuum, ε_r the dielectric constant of water, T the absolute temperature, N_A the Avogadro number, k the Boltzmann constant, c_i the local concentration of ion i and c_0 the water concentration.

The entropy of mixing the different amphiphilic molecules in the aggregates contributes considerably to the free energy of the system. We will approximate this entropy by the expression for ideal mixing

$$-TS_{agg}=kT\sum n_a \ln X_a, \tag{3}$$

where n_a and X_a are respectively the number and the number fraction of the different amphiphile molecules.

It is an experimental observation that the interfacial energy of the aggregates is simply proportional to the aggregate/water contact area for lamellar phases in many different surfactant systems [9]. The proportionality constant, γ, is approximately 18 mJ m^{-2}, and we have used this value for all three aggregate geometries, even though one might argue that the value of γ should depend slightly on the curvature of the surface of the aggregate, and on A_{sp}. However, this is not a serious matter, since our interest is focused on the general trends concerning the formation of ribbon phases, and not on describing phase diagrams corresponding to specific systems in detail. The interfacial energy will thus contribute with a term

$$G_s=\gamma\sum n_a A_{sp} \tag{4}$$

to the free energy of the system.

As mentioned above, there are no intrinsic aggregate entropies included in the calculations, i.e. the aggregates are considered to be stiff and of mono-disperse size distribution. At short inter-aggregate distances there is a repulsive force between the aggregates, sometimes referred to as 'the hydration force'. This force decays approximately exponentially with a decay length of about 2–4 Å [29, 30] and would therefore not contribute significantly to the free energy of the system at the concentrations of interest here (surfactant concentrations, $c_s \approx 60$ wt.%, or smaller); hence this force is not included in the calculations. Finally, the energy connected with the van der Waals force will not be considered in the calculations, as this force is of importance only in the most water rich parts of the phase diagram. It is important to note that there are no fitting parameters in the model presented.

The chemical potential for the different components are calculated by direct differentiation of the free energy expressions. These have been derived for aggregates

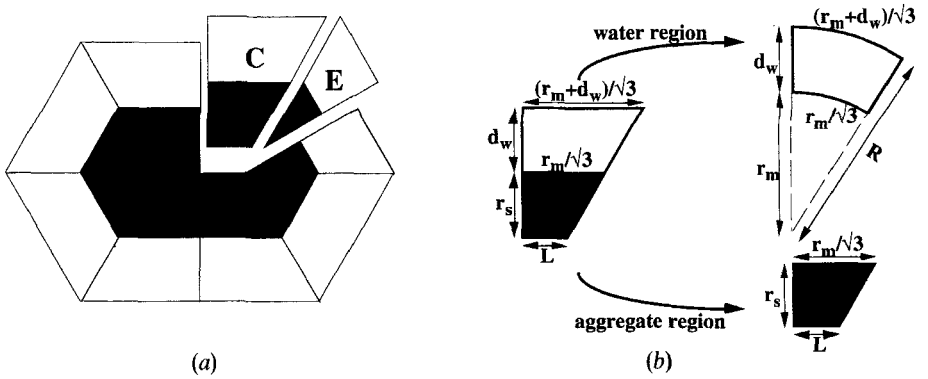

(*a*) (*b*)

Figure 7. (*a*) The asymmetric hexagon is divided into 4 central sub-systems (C) and 8 edge sub-systems (E). (*b*) The water region with tetragonal symmetry is approximated by a circular cylindrical system, where $r_m=r_s+L\sqrt{3}$. The water volume as a function of the distance from the aggregate surface is the same for the two different symmetries. Note that the sub-system E is the special case of the sub-system C, when $L=0$.

with circular cylindrical symmetry and lamellar symmetry in [9, 11], and subsequently we have used these expressions for the regular hexagon cylinders and the bilayers in our calculations.

We have derived the expressions for the chemical potentials of the different components for the case of the asymmetric hexagon cylinders, copies of this work, which comprises 9 pages, may be obtained from the British Library, Lending Division, by quoting the number SUP 16528 according to the procedure described at the end of this issue. The asymmetric hexagon cylinders are divided into 12 parts with two different geometries (C and E), as shown in figure 7. Both types of sub-system are assumed to have circular cylindrical symmetry for the water region of the cells and the solutions to the Poisson–Boltzmann equation for the circular cylindrical symmetry are therefore used also for this case.

3.2. *The computational procedure*

The computational procedures to calculate the phase diagram and the dimensions of the aggregates are as follows: (i) The chemical potentials for all components are calculated for the cylindrical system with specified composition, temperature and aggregate dimensions. The procedure is repeated with new values for the dimensions of the aggregates until the aggregate dimension that minimizes the free energy of the system is obtained. The finally obtained aggregates may have normal sections like that of symmetric hexagons with $r_s \leqslant r_{max}$ and $L=0$, or like that of asymmetric hexagons with $r_s = r_{max}$ and $L>0$. A new set of composition and temperature is then chosen if the aim is to investigate the dimensions of the cylindrical aggregates. If, on the other hand, the goal is to investigate the boundary to the lamellar phase, the calculation continues as follows: (ii) The chemical potentials of the components for a lamellar system, which has the same chemical potential of the water as that obtained for the cylindrical system, is calculated. The lamellar thickness and the composition of the system for which the free energy is at a minimum is determined. (iii) The most stable phase is identified. Points in the phase diagram, for which the chemical potentials of all components have the same values for the cylindrical region as for the lamellar region, are end-points of the tie-lines of the two-phase region that separates these regions.

4. Predictions of the model and comparisons with the experimental results

In what follows, we will present some predictions of the thermodynamic model presented above. We start by presenting the calculated dimensions of the aggregates and proceed with the phase diagrams. We then summarize the results (table 4), and finally make comparisons with the experimental observations.

4.1. *Theoretical results*

We have calculated to what extent the dimensions of the aggregates with normal cylindrical symmetry are affected by changes in temperature and composition. The parameters for the surfactant molecule are as those for a potassium palmitate molecule [7], i.e. with mass 295 g mol^{-1} and volume $V_s/\text{Å}^3 = 467 + 0{\cdot}368^*(T\text{-}298)$ per amphiphile, where T is the absolute temperature. The smallest dimension of the aggregates is smaller than, or equal to r_{max}, which was chosen to be 18 Å, or about 80 per cent of l_{at}. The results from the calculations are displayed in figure 8, where the lines represent points in the temperature–composition plane for which the axial ratio of the aggregates is at a constant value. For smaller/bigger values of r_{max} these lines are shifted to the left/right in the diagram.

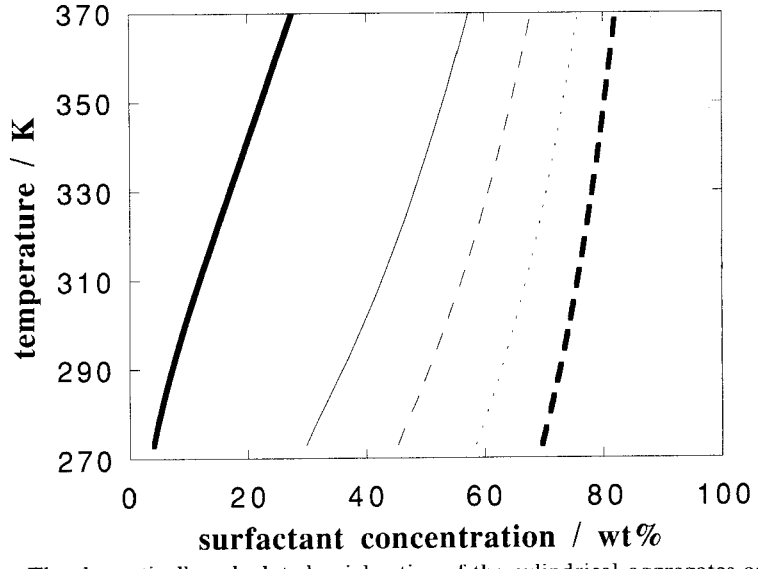

Figure 8. The theoretically calculated axial ratios of the cylindrical aggregates are constant along the presented lines in the temperature/composition diagram. (————), $\rho = 1{\cdot}0$; (——), $\rho = 1{\cdot}1$; (– – –), $\rho = 1{\cdot}2$; (- - - -), $\rho = 1{\cdot}4$; (— — —), $\rho = 2{\cdot}0$.

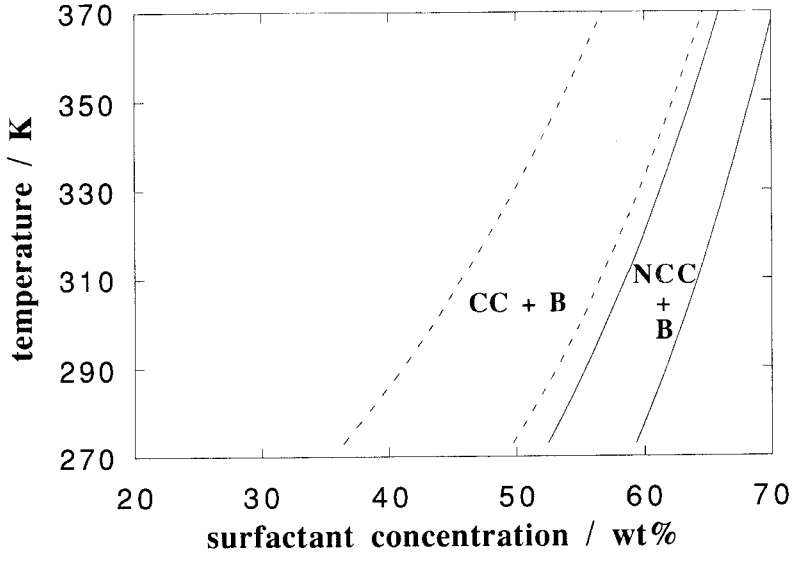

Figure 9. Theoretically calculated temperature/composition phase diagram. The dotted lines represent the two phase region between the phases with circular cylinders (CC) and bilayers (B), whereas the full lines represent the two phase region between the phases with non-circular cylinders (NCC) and bilayers (B). The parameters which are used in the calculations are given in the text.

Next the transition from the cylindrical region to the lamellar region is investigated, and with the same parameters as used when obtaining figure 8, the phase diagram of figure 9 is obtained (solid lines). The transition is first order, with a two-phase region of about 5 wt%. As a comparison, the transition from the cylindrical region with aggregates for which L is fixed to zero, to the lamellar region is also displayed in figure 9 (dotted lines). The cylindrical phase is stable at 10–15 wt% higher surfactant concentrations when $L \geqslant 0$ than for the case when $L=0$, and the cylindrical region is favoured when the aggregates have the possibility of growing asymmetrically. The two-phase regions are shifted towards lower/higher surfactant concentrations for smaller/bigger values of r_{max}.

In order to investigate the effect of surfactant headgroup charge on the formation of asymmetric cylindrical aggregates, we have calculated the phase diagram for a surfactant with a variable headgroup charge. We have used the same molecular parameters as those for the DA + z/D_2O system [7]. The dissociation constants for the amphiphilic molecule are $K_{a1}=K_{a2}=10^{-10}$ in the absence of electric fields. The molar mass of the surfactant is $(242+36z)$ g, the volume is 500 Å^3 per amphiphile molecule and $r_{max}=17{\cdot}3$ Å, or about 80 per cent of l_{at} for this amphiphilic molecule. The calculations have been performed for surfactant average charges between +0·8 and +2·0, and the phase diagram is represented with the surfactant(+2), the surfactant(+0) and water as the three components (figure 10). The dotted lines in figure 10 represent the lines for which the axial ratio of the aggregates is constant at 1 : 1 (and with $r_s=r_{max}$) and 1·5 : 1 respectively. The main features of the calculations are listed in table 4.

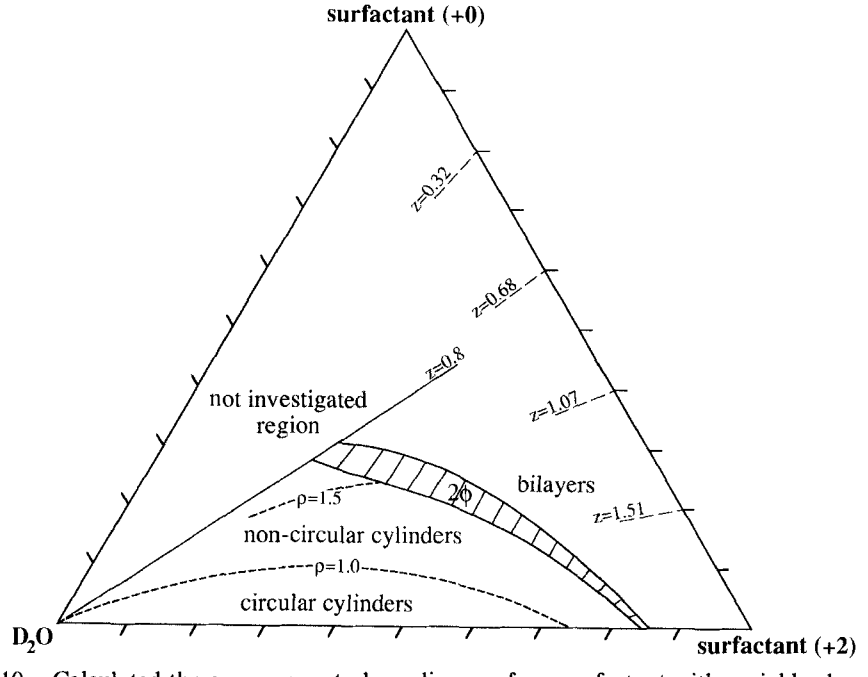

Figure 10. Calculated three component phase diagram for a surfactant with variable charge (pH-dependent) and water as the components. The thin, solid lines are tie-lines between the phase with cylindrical aggregates and the phase with bilayer-like aggregates. The region with surfactant average charges bigger than +0·8 has been investigated. The parameters which are used in the calculations are given in the text.

4.2. *Comparisons between the experimentally and theoretically obtained results*

By a comparison of the experimentally and theoretically derived statements {1}, {2}, {4–6} and {10–12} of table 4, it is clear that the model describes the transition from the hexagonal phase (with circular cylinders) to the lamellar phase quite successfully. The trends for the phase sequence, and the growth of the aggregates, when the surfactant concentration increases, are two features well described by the model. However, in some respects the model fails to predict the experimentally obtained data. Thus the model predicts that the asymmetric growth of the cylinders starts at rather low surfactant concentrations {7}, and that the so formed cmm phase exists over a wide range of concentration {7}, at all temperatures of interest {8}, and for all surfactant/water systems {9} (that is, for all single chain, ionic surfactants). One can proceed in two ways to deal with this state of affairs.

The first, and (perhaps) simplest way is to consider these contradictions ({7–9} in table 4) as consequences of the simplicity of the model. Recall that the model does not rely on any fitting parameters. One could introduce fitting parameters, for example, by dividing the cylindrical region into one phase with circular cylinders with $r_{max} = l_{at}$ and one phase with ribbon-like cylinders with $r_s = 0{\cdot}8\, l_{at}$. By then letting γ vary with temperature and surfactant concentration in an appropriate way, the experimentally obtained phase diagrams could be matched. We are reluctant to perform such an analysis, since it does not give a better understanding of the properties of ribbon phases.

Instead, we find it more worthwhile to search for the weak points in the theoretical approach. The calculations for the cylindrical region are performed in a cell model, where the cells are hexagon-like, and therefore the phase symmetry changes from p6m to cmm immediately as L becomes non-zero. However, one could argue that the hexagonal symmetry of the phase is retained even though L is non-zero (see further discussion below). If this is the case, it follows that the cylindrical aggregates have non-circular normal sections at surfactant concentrations that are well below those for which the ribbon phases are obtained experimentally, i.e. in big regions of the hexagonal phases. Thus it is possible that the model predictions of the aggregate dimensions are reliable, whereas one has to treat the model predictions of the phase structure with caution. In order to check the validity of this suggestion, we will investigate the experimental data obtained for phases with hexagonal structure.

The hexagonal symmetry is conveniently established by SAXS measurements, but unfortunately very little can be said about the shape of the aggregates from these data. Since the normal sections of the cylinders have to possess an axis of rotation with six-fold symmetry in order to be consistent with the p6m space group [31], one has simply assumed that the normal sections of the aggregates are circular. There is however the possibility that the cylinders are asymmetric, but that the average shape of the aggregates is that of circular cylinders. Hendrikx and Charvolin have suggested that this is the case in parts of the hexagonal phase in the sodium decylsulphate/1-decanol/water system [18, 27]. They used a technique, based on small angle neutron scattering (SANS) measurements, to get a direct measure of the distribution of the decanol molecules and the decylsulphate molecules in the aggregates. Aggregates with stiff, circular cylinders were, according to Hendrikx and Charvolin, not consistent with the scattering data, and their conclusion was that the normal sections of the aggregates therefore are non-circular, and they proposed that the needed (six-fold) symmetry of the aggregates is obtained through an orientational disorder of the aggregational normal section along their axes, as indicated in figure 11. There are also SAXS measurements for hexagonal phases that indicate, though indirectly, the existence of ribbon-like

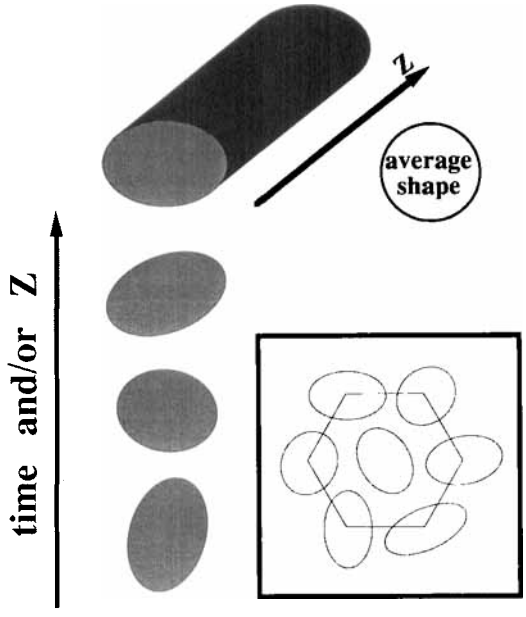

Figure 11. An attempt to picture the asymmetric, fluctuating, aggregates of the hexagonal phase. The degree and the orientation of the deformation of the aggregates varies along the rod and with time, so that the shape of the normal sections is circular on average.

aggregates. Kékicheff and Cabane [3] obtained diffuse scattering around the central Bragg peaks for a sample in the hexagonal region of the SDS/water system. The presence of asymmetric aggregates is consistent with this observation. It has also been claimed that $r > l_{at}$ (assuming circular cylinders) for regions of the hexagonal phases in some systems [18, 27, 32], which would support the existence of non-circular cylinders in the hexagonal region. However, our calculations of the radii of the (assumed circular) aggregate normal sections from the same data, evaluated for the hydrocarbon core of the aggregates, show that $r_{hc} \approx l_{at}$, or smaller, for all cases [33]. Nevertheless, the aggregates of these samples may be non-circular, since it may well be that $r_{max} < l_{at}$ for the cylindrical aggregates.

To conclude, there are no inconsistencies between the experimentally and theoretically derived statements, {7–9} of table 4, if we allow the aggregates of the experimentally obtained hexagonal phases to have non-circular normal sections (with $r_s < \approx l_{at}$), and allow the theoretically obtained non-circular aggregates to pack on a hexagonal lattice.

5. Concluding discussion

In this section, we discuss the driving mechanisms behind the transition from the hexagonal phase to the lamellar phase. In doing so we will consider the experimental and theoretical results that are presented in table 4 and which are further discussed in the previous section. However, it will be shown that the knowledge about the transition from the micellar solution phase to the hexagonal phase also provides an important clue in order to understand these matters. The following discussion leads to the schematic phase and aggregate diagram for single-chain, ionic surfactant/water systems which is presented in figure 12.

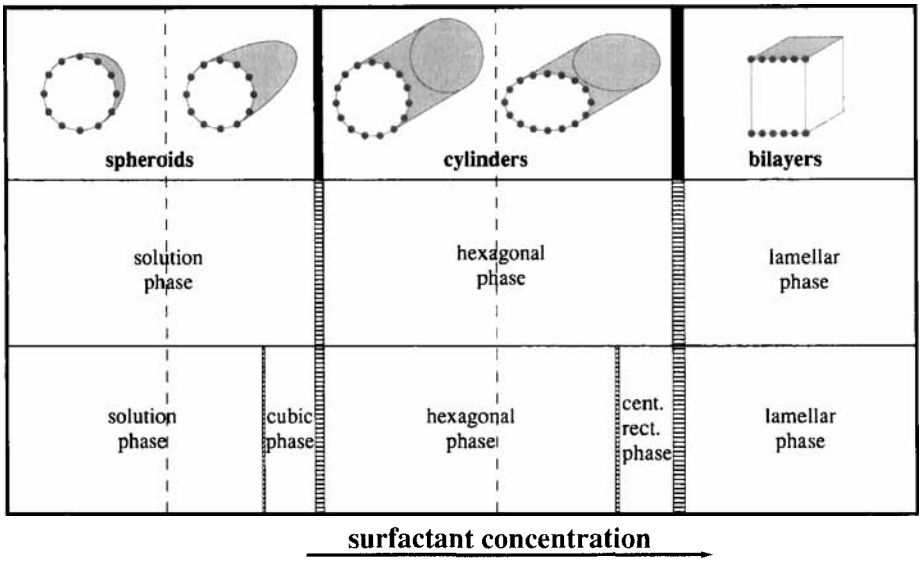

Figure 12. Typical phase and aggregate diagrams for single-chained, ionic surfactant/water systems. The hatched areas represent two-phase regions.

5.1. *Aggregational growth—from sphere to bilayer*

There are three principal aggregate structures found in charged surfactant/water systems, namely spheres, circular cylinders of infinite length and bilayers of infinite extension in two dimensions. The higher the curvature of the aggregates, the bigger is the available area for each surfactant headgroup, which, due to restrictions in the packing of the amphiphilic molecules, is typically 75 Å^2 for a sphere, 50 Å^2 for a cylinder and 25 Å^2 for a bilayer. It is an experimental fact that spheres are obtained at high water concentrations and lamellae at low water concentrations, whereas cylinders form at intermediate water concentrations. This observation is an effect of the fact that the counter-ion screening of the electrostatic potential of the aggregate surfaces increases when the amount of water in the system decreases (for entropic reasons). Since the water fraction decreases monotonically, one would expect A_{sp} to decrease monotonically as well, and this is achieved by an increase in aggregate size. The growth may be symmetric, in the sense that the smallest dimension of the aggregates increases (within each aggregate symmetry) when the water fraction decreases, or asymmetric. The most familiar type of asymmetric aggregational growth is the growth from spherical micelles to prolate-like micelles, a process which is a general property for ionic, single-chain, surfactant/water systems [34]. The asymmetric growth from circular cylinders to ribbon-like cylinders is analogous, and therefore we propose that the deformation to non-circular cylinders, when the water fraction of the system decreases, is also a general phenomenon. The predictions of the Poisson–Boltzmann cell model are in support of this proposal (see table 4).

5.2. *Phase structure—from the micellar solution phase to the lamellar phase*

It is a fact that changes of the aggregational shape do not necessarily affect the structure of the phase. The most well-known example is a micellar solution phase where the aggregates may be spherical, as well as prolate-shaped. In analogy with this

experimental fact, the existence of asymmetric aggregates in phases with hexagonal symmetry, as proposed by Fontell *et al.* [32] and Hendrikx and Charvolin [18, 27], seems reasonable. We propose that the cylindrical aggregates of the hexagonal phases generally have non-circular normal sections in the more concentrated regions, i.e. the regions that are close to the adjacent phase at higher surfactant concentrations. This proposal is based on two observations. The first is that the formation of solution phases with asymmetric aggregates (prolate-like micelles) appears to be a general phenomenon for ionic surfactant/water systems, and that there seems to be no reason why the formation of hexagonal phases with asymmetric aggregates (ribbon-like cylinders) should be less general. The second is that the thermodynamic model predicts that the asymmetric growth of the cylindrical aggregates starts at low surfactant concentrations, well below those where the lamellar phase is obtained.

The asymmetry of the cylindrical aggregates increases when the water fraction of the system decreases, and finally the aggregates can no longer be packed on a hexagonal lattice. For the majority of systems lamellar phases are then obtained. However, occasionally the asymmetric aggregates pack on a centred rectangular lattice before the lamellar phase (or other intermediate phases) is obtained, and in order to rationalize this observation the knowledge about the transition from spheres to cylinders will again prove useful. It has been concluded that prolate micelles form solution phases. This is possible only for micelles that are orientationally (as well as translationally) disordered, due to aggregational tumbling and/or fluctuations of the dimensions of the aggregates. There is both experimental and theoretical evidence for the fact that the aggregates of these micellar solutions have substantial shape polydispersity and fluctuations [34, 35]. The free energy cost for the shape fluctuations is quite small, in the order of $kT/100$ per surfactant molecule [34]. As soon as the aggregates get ordered, a phase transition is obtained. The resulting phase has a nematic structure when the prolate-like micelles order orientationally [36], and has a cubic symmetry when the micelles order translationally [6, 37]. The nematic and discrete cubic phases are obtained at surfactant concentrations between those of a micellar solution phase and a hexagonal phase. Similarly, the hexagonal packing of the ribbon-like cylinders is possible only when the average shape of the aggregates is that of a circular cylinder, due to fluctuations of the orientation of deformation, as well as the degree of deformation, along the axis of the aggregates and/or with time. When the deformed cylinders orient with respect to each other, phases with lower than hexagonal symmetry are obtained, located intermediate between the hexgonal and lamellar phases in the phase diagrams. A centred rectangular symmetry has been established experimentally for these phases [7], but other symmetries are possible.

5.3. *The mechanisms behind the formation of the centred rectangular ribbon phases*

We propose that the mechanism for the transition from the hexagonal phase, with asymmetric aggregates to the rectangular ribbon phase is as follows. On the one hand the hexagonal phase is entropically stabilized as compared to the rectangular phase, due to the internal aggregate entropy, which is connected to the fluctuations of the dimensions of these aggregates. On the other hand, the rectangular structure is enthalpically stabilized as compared to the hexagonal structure, which is partly due to the fact that the hydrophilic/hydrophobic area is smaller for a stiff ribbon-like aggregate than for a fluctuating, 'twisted' ribbon-like aggregate, but also due to the fact that the electrostatic energy is smaller for the rectangular phase. This follows, since the thickness of the interaggregate water layer differs markedly for the hexagonal phase

with fluctuating asymmetric aggregates, but is approximately constant in the rectangular phase. The transition from the hexagonal phase with fluctuating asymmetric aggregates to the rectangular phase with stiff ribbon-like aggregates is therefore of the disorder–order type. Moreover, partial ordering of the hexagonal aggregates is not possible, and the phase transition is of the first order. The two-phase regions have however rather limited extensions, since the aggregate dimensions are similar in the two phases. This may be the explanation for why no two-phase regions for this phase transition have been observed for the SDS/water system (at elevated temperatures) and the CsMy/water system (figure 1). The disappearance of the centred rectangular phases at elevated temperatures is in line with the argument that this phase structure is entropically destabilized as compared to the hexagonal structure. However, the fact that the axial ratio of the aggregates slightly decreases when the temperature increases is also of importance for this phase behaviour.

Appendix A

For a two-dimensional, centred rectangular lattice the Bragg spacings are [31]

$$d_{hk}=\left(\frac{h^2}{a^2}+\frac{k^2}{b^2}\right)^{-1/2}, \tag{A 1}$$

with the restriction that $h+k=2n$, where n is an integer, h and k are the Miller indices for the plane, and a and b are the dimensions of the unit cell (see figure 2). Within the hexagon–rod model [7] (see figure 3), the smallest dimension of the aggregates is then calculated according to

$$r_s=-\frac{L}{\sqrt{3}}+\sqrt{\left(ab\phi\frac{\sqrt{3}}{12}+\frac{L^2}{3}\right)}, \tag{A 2}$$

where a and b are the unit cell dimensions, ϕ is the aggregate volume fraction and L is half the length of the lamellar-like parts of the hexagon

$$2L=\tfrac{1}{2}(a-b\sqrt{3}). \tag{A 3}$$

The axial ratio of the aggregate normal section is then defined as

$$\rho=1+\frac{L}{r_s}. \tag{A 4}$$

We will use the hydrocarbon volume fraction as the aggregate fraction, ϕ, in the calculations. The reason for this is that the hydrocarbon core of the aggregates is rather homogeneous (i.e. it contains no water molecules or counter-ions), whereas there are an unknown number of water molecules and counter-ions in the headgroup region. For a system with a surfactant (s), a cosurfactant (c) and water (w), the hydrocarbon volume fraction is calculated according to

$$\phi_{hc}=\frac{V_{s,hc}+(n_c/n_s)V_{c,hc}}{V_s+(n_c/n_s)V_c+(n_w/n_s)V_w}, \tag{A 5}$$

n_x/n_s is the number of molecules x per amphiphile molecule in the sample, V_x is the volume of molecule x and $V_{x,hc}$ denotes the volume of the hydrocarbon part of molecule x.

The volumes that we have used in equation (A 5) are the ones that are given in [7]. All SAXS data are evaluated by the hexagon–rod model, including those samples in the SdS/dec/water system that, according to [27], are of pgg symmetry.

Appendix B

The relationship between the axial ratio, ρ, and the asymmetry parameter, η, as obtained by NMR measurements is derived in [7] for the case of the hexagon–rod model and the binary surfactant/water system. Here we will investigate also a three component system (KP/KL/water) and we will thus generalize the model to this situation. For slightly deformed aggregates (the small deformation regime), and for the case when the area per polar headgroup is constant over the surface of the aggregates, the axial ratio of the aggregate normal section is

$$\rho = 1 + \sqrt{3}\frac{\eta_1 X_1 + \eta_2(1-X_1)}{3-\eta_1 X_1 - \eta_2(1-X_1)}, \tag{B 1}$$

where X_1 is the mol fraction of the amphiphilic compound of type 1, and η_1 and η_2 are the asymmetry parameters for the two surfactant molecules, respectively.

References

[1] Luzzati, V., Mustacchi, H., Skoulios, A. E., and Husson, F., 1960, *Acta crystallogr.*, **13,** 660.
[2] Husson, F., Mustacchi, H., and Luzzati, V., 1960, *Acta crystallogr.*, **13,** 668.
[3] Kékicheff, P., and Cabane, B., 1987, *J. Phys., Paris*, **48,** 1571.
[4] Anderson, D. M., 1990, *J. Phys., Paris, Colloque C*, **7,** 1.
[5] Henriksson, U., Blackmore, E. S., Tiddy, G. J. T., and Söderman, O., 1992, *J. phys. Chem.*, **96,** 3894.
[6] Fontell, K., 1990, *Colloid Polym. Sci.*, **268,** 264.
[7] Hagslätt, H., Söderman, O., and Jönsson, B., 1992, *Liq. Crystals*, **12,** 667.
[8] Balmbra, R. R., Bucknall, D. A. B., and Clunie, J. S., 1970, *Molec. Crystals liq. Crystals*, **11,** 173.
[9] Jönsson, B., 1981, Thesis, University of Lund.
[10] Jönsson, B., and Wennerström, H., 1981, *J. Colloid Interface Sci.*, **80,** 482.
[11] Jönsson, B., and Wennerström, H., 1987, *J. phys. Chem.*, **91,** 338.
[12] Landgren, M., 1990, Thesis, University of Lund.
[13] Chidichimo, G., Raudino, A., and Imbardelli, D., 1990, *Coll. Surf.*, **49,** 303.
[14] Ekwall, P., Mandell, L., and Fontell, K., *J. Colloid Interface Sci.*, **31,** 508.
[15] Chidichimo, G., Vaz, N. A. P., Yaniv, Z., and Doane, J. W., 1982, *Phys. Rev. Lett.*, **49,** 1950.
[16] Benigni, S., and Spelberg, N., 1987, *Molec. Crystals liq. Crystals*, **150b,** 301.
[17] Alpérine, S., Hendrikx, Y., and Charvolin, J., 1985, *J. Phys. Lett., Paris*, **46,** 27.
[18] Hendrikx, Y., and Charvolin, J., 1988, *Liq. Crystals*, **3,** 265.
[19] Hendrikx, Y., and Charvolin, J., 1981, *J. Phys., France*, **42,** 1427.
[20] Auvray, X., Petipas, C., Anthore, R., Rico, I., and Lattes, A., 1989, *J. phys. Chem.*, **93,** 7458.
[21] Auvray, X., Perche, T., Anthore, R., Petipas, C., Rico, I., and Lattes, A., 1991, *Langmuir*, **7,** 2385.
[22] Kang, C., Söderman, O., Eriksson, P. O., and Stael von Holstein, J., 1992, *Liq. Crystals*, **6,** 71.
[23] Wood, R. M., and McDonald, M. P., 1985, *J. chem. Soc. Faraday Trans. I*, **81,** 273.
[24] Blackburn, J. C., and Kilpatrick, P. K., 1992, *Langmuir*, **8,** 1679.
[25] Blackburn, J. C., and Kilpatrick, P. K., 1992, *J. Colloid Interface Sci.*, **149,** 450.
[26] Vaz, N. A. P., and Doane, J. W., 1980, *Phys. Lett.*, **77A,** 325.
[27] Hendrikx, Y., and Charvolin, J., 1992, *Liq. Crystals*, **11,** 677.
[28] Ekwall, P., 1975, *Advances in Liquid Crystals*, Vol. 1, edited by G. H. Brown (Academic Press), p. 1.
[29] Rand, R. P., 1981, *A. Rev. Biophys. Bioengng*, **10,** 277.
[30] Jönsson, B., and Wennerström, H., 1983, *J. chem. Soc. Faraday Trans. II*, **79,** 19.
[31] 1952, *International Tables for X-ray Crystallography*, Vol. 1 (The Kynoch Press), p. 1.

[32] FONTELL, K., MANDELL, L., LEHTINEN, H., and EKWALL, P., 1968, *Acta polytech. scand., Chem. Incl. Metall. Ser.*, **74III,** 1.
[33] HAGSLÄTT, H. (unpublished results) 1992.
[34] HALLE, B., LANDGREN, M., and JÖNSSON, B., 1988, *J. Phys. France*, **49,** 1235.
[35] CABANE, B., DUPLESSIX, R., and ZEMB, T., 1985, *J. Phys., France*, **46,** 2161.
[36] SONIN, A. S., 1987, *Soviet Phys. Usp.*, **30,** 875.
[37] FONTELL, K., FOX, K. K., and HANSSON, E., 1985, *Molec. Crystals liq. Crystals*, **1,** 9.
[38] CHIDICHIMO, G., GOLEMME, A., DOANE, J. W., and WESTERMAN, P. W., 1985, *J. chem. Phys.*, **82,** 536.
[39] KÉKICHEFF, P., GRABIELLE-MADELMONT, C., and OLLIVON, M., 1989, *J. Colloid Interface Sci.*, **131,** 112.
[40] HAGSLÄTT, H., and FONTELL, K., *J. Colloid Interface Sci.*, (in the press).
[41] KANG, C., and SÖDERMAN, O., 1991 (unpublished results).